



Trade Science Inc.

Nano Science and Nano Technology

An Indian Journal

Full Paper

NSNTAJ, 3(2), 2009 [21-27]

Growth and photoluminescence of SnO₂ nanoleaves and nanopencils synthesized by Au-Ag alloying catalyst assisted carbothermal evaporation

B.Wang¹, G.Ouyang^{2,*}, I.L.Li¹, P.Xu¹
¹Shenzhen Key Laboratory of Micro-Nano Photonic Information Technology, School of Electric Science and Technology, Shenzhen University, Shenzhen 518060, (CHINA)

²Key Laboratory of Low-Dimensional Quantum Structures and Quantum Control of Ministry of Education, and Department of Physics, Hunan Normal University, Changsha 410081, (CHINA)

E-mail: gangouy@hunnu.edu.cn

Received: 12th July, 2009 ; Accepted: 22nd July, 2009

ABSTRACT

SnO₂ nanoleaves and nanopencils have been synthesized on single silicon substrates using Au-Ag alloying catalyst assisted carbothermal evaporation. The products were characterized with field-emission scanning electron microscopy (FESEM), X-ray diffraction (XRD), Raman spectra, and photoluminescence spectra (PL). In comparison with SnO₂ nanopencils, the new peak at 456 nm in the measured PL spectra of SnO₂ nanoleaves is observed, implying that more luminescence centers exist in these nanostructures. The possible growth mechanisms are discussed for the nanoleaves and nanopencils. Based on the detailed characterization results, we can conclude that the diffusion behavior of surface atoms under different ambient conditions and the different supersaturating degree of alloying droplets would be responsible for the formation of different morphologies of SnO₂ nanostructures. © 2009 Trade Science Inc. - INDIA

KEYWORDS

Characterization;
Low dimensional structures;
Nanostructures;
SnO₂.

INTRODUCTION

It is well known that the large ratio of surface-to-volume and the coordination numbers imperfection of surface atoms of one-dimensional (1D) nanostructured materials have stimulated intensive interest in mesoscopic physics and material science, which not only provide a sort of good system to investigate the electrical and thermal transport in 1D confinement, but also are expected to play an important role in both interconnection and functional units in fabricating electronic, optoelectronic, and magnetic storage devices in nanoscale dimension^[1-4]. In

general, SnO₂ ($E_g = 3.54$ eV, at 300 K) is an important functional material, which has been widely applied in the field of nano- and microelectronics, such as solar cells^[5], transparent conducting electrodes^[6], gas sensors^[7,8], and transistors^[9], etc. Naturally, to obtain SnO₂-based nanoscaled devices, we meet the great challenge that we need try to prepare various nanoscaled building blocks from zero to three dimensions, e.g., particles, tubes or wires, and belts or junctions, etc. Thus, the assembly, synthesis and related physical properties of zero- and 1D SnO₂ nanostructures such as particles^[10-12], tubes^[13], and

Full Paper

wires^[14-23] have been attracted intensive attention in recent years. For example, a α -Sn nanowire confined in a SnO₂ nanotube with core-shell configuration shows the giant superheating behavior under high temperature, confirming by *in situ* transmission electron microscopy observations^[24]. Evidently, the surface and interface effect would be largely influenced on physical properties of nanostructures^[25-28]. However, in comparison with other SnO₂ nanostructures, there only a few studies pay attention to two-dimensional (2D) nanostructures such as nanosheets^[29]. In fact, 2D SnO₂ nanostructures could be found to possess the unique applications in gas sensors, energy storage, memory devices, and as electrodes for fuel cells, etc^[30,31]. Therefore, in this contribution, we report that the difference of two kinds of SnO₂ nanostructures, including 2D nanoleaves and 1D nanopencils, have been synthesized on Au-Ag covered Si substrates using thermal evaporation of active carbon and SnO₂ powders. Furthermore, the growth mechanism and photoluminescence behaviors have also been discussed.

EXPERIMENT

The schematic diagram of the apparatus used in our experiment is shown in Figure 1. First of all, the Au-Ag (atom ratio 1:1) layer (about 10 nm in thick-

ness) is deposited on single silicon (001) substrates with area of 5 mm² by sputtering. The active carbon and SnO₂ powders (both 99.99%) are mixed in a 1:4 weight ratio and placed into a small quartz tube. Two Si substrates covered by Au-Ag alloy are put on a ceramic plate near the mixture inside the small quartz tube. The distance between two substrates is about 2 cm, while the substrate 1 is 1 cm away from the mixture. Then, the small quartz tube with inner diameter of 2.5 cm is pulled into the center of the large one with inner diameter of 6 cm. They are together inserted in a horizontal tube electric furnace. The whole system is evacuated by a vacuum pump for a couple of hours, and then, the pure nitrogen gas is guided into the system at flow rates in 250 sccm under the pressure of 700 Torr. Afterwards, the system is rapidly heated up to 900 °C (the temperature in the place of the electric couple) from the room temperature and be kept at the temperature for 10 min. The temperature in the substrate 1 is higher than that of the substrate 2 because the distance between the substrate 1 and the electric couple is nearer than the distance between the substrate 2 and the electric couple. Finally, the system is cooled down to the room temperature over several hours. When two substrates are taken from the small quartz, we can see some gray productions on substrates.

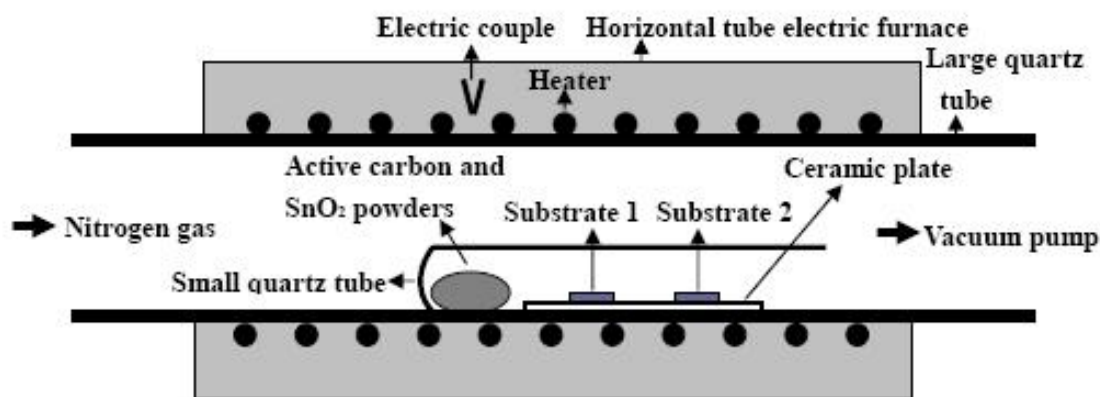


Figure 1: Schematic diagram of apparatus used in the experiment.

Synthesized material was employed by FESEM, XRD and Raman spectrum to characterize the morphology and structure. Room-temperature PL is used to identify the luminescence behavior. Note that we can easily repeat the experimental results, suggesting that our method is flexible and reproducible.

RESULTS AND DISCUSSION

Morphologies of the synthesized SnO₂ nanostructures in two substrates are, respectively, shown in Figure 2 and Figure 3. It is clearly to see that many SnO₂

nanoleaves in substrate 1 shown in Figure 2 (a). Also, the magnified FESEM image is displayed in Figure 2 (b). In detail, four SnO_2 nanoleaves with stipe and vein are clearly shown, which the vein includes three-dimensional space sizes of length, width and thickness. The range of size in length and thickness of the veins is, respectively, 4-5 μm and 100-200 nm, while the width transits 500-

800 nm in the root and 30-50 nm in the tip. The diameter of the stipe is about 100-150 nm. Figures 2(c) and 2(d) show the FESEM image of one SnO_2 nanoleave and the corresponding higher magnified FESEM image. Clearly, we can see the width of the root of vein and the thickness are about 500 nm and 150 nm, respectively. The diameter of the stipe with circle-shape is about 120 nm.

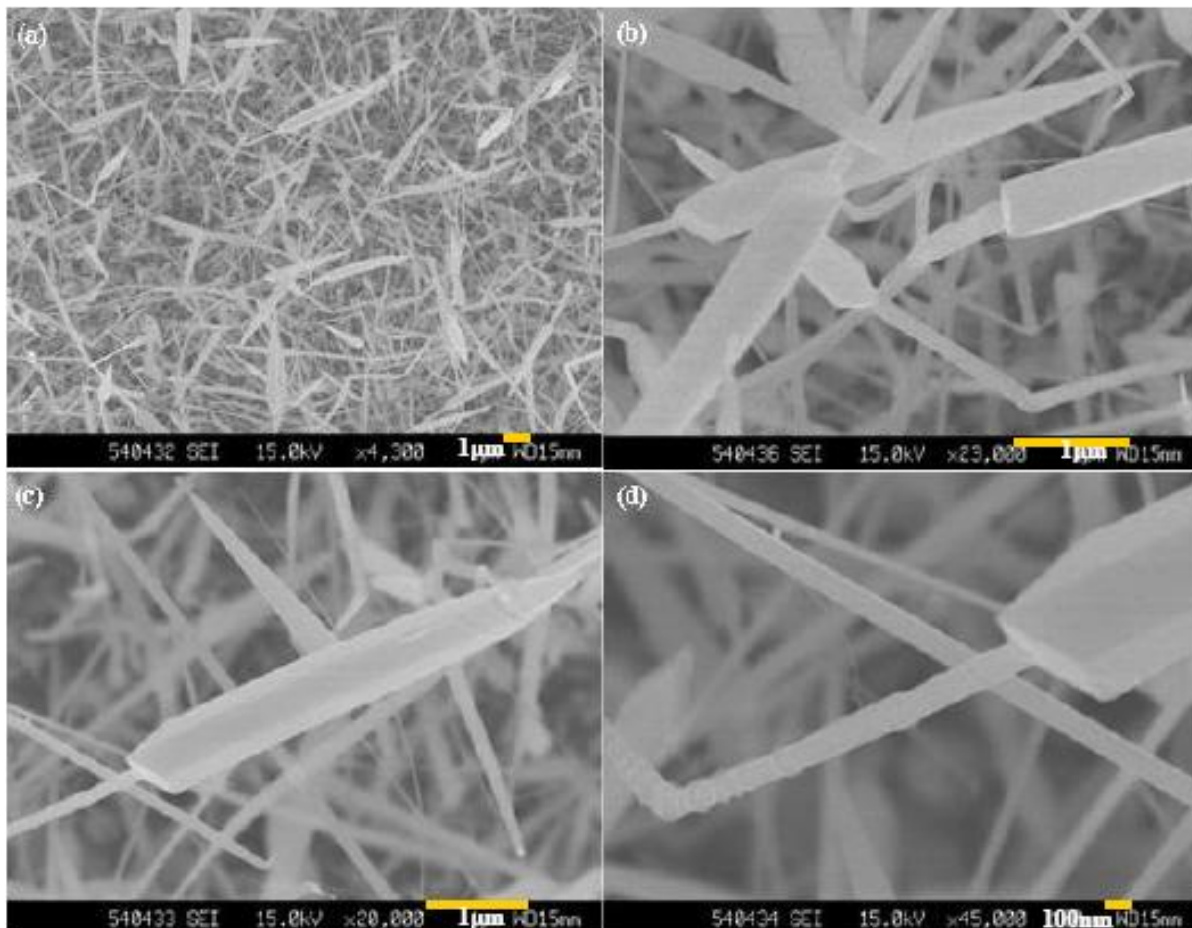


Figure 2 : FESEM morphologies (a), (b), (c), (d) of the synthesized SnO_2 nanoleaves.

On the other hand, a number of SnO_2 nanopencils found in substrate 2 with the length of 8-10 μm are displayed in Figure 3(a). Meanwhile, Figure 3(b) displays the magnified FESEM images of two SnO_2 nanopencils, which indicates that their shape can be involved in two parts: body and tip. Interestingly, we can see the size of nanopencils becomes wider slowly along the body section, and then turns thinner quickly along the tip part. More specifically, Figure 3(c) shows the cross section of the body is square-shape, while the border length of the cross section transits from 100 nm to 500 nm slowly along the body. The higher-magnified FESEM image of the tip part shown in Figure 3 (c) is

displayed in Figure 3 (d). However, we found that the cross section of the tip part is circular-shape, while the diameter of the cross section transits from 500 nm to 30 nm quickly along the tip.

The XRD measurement is carried out to identify the crystalline structure of two kinds of SnO_2 nanostructures, as shown in Figure 4. Clearly, both SnO_2 samples show a tetragonal rutile SnO_2 phase with (110), (101), (200), (111), (211), (220), (002), (310), (112), (301), (202) and (321) diffraction peaks. So, the XRD patterns of the samples can be indexed to the tetragonal rutile structure of SnO_2 with lattice constants of $a = 0.4738$ nm and $c = 0.3188$

Full Paper

nm (JCPDS 21-1250). The intensity of the peak in XRD pattern of nanoleaves is higher than that of nanopencils because the thickness and the density of

the nanostructures synthesized in substrate 1 are higher than those of the nanostructures synthesized in substrate 2.

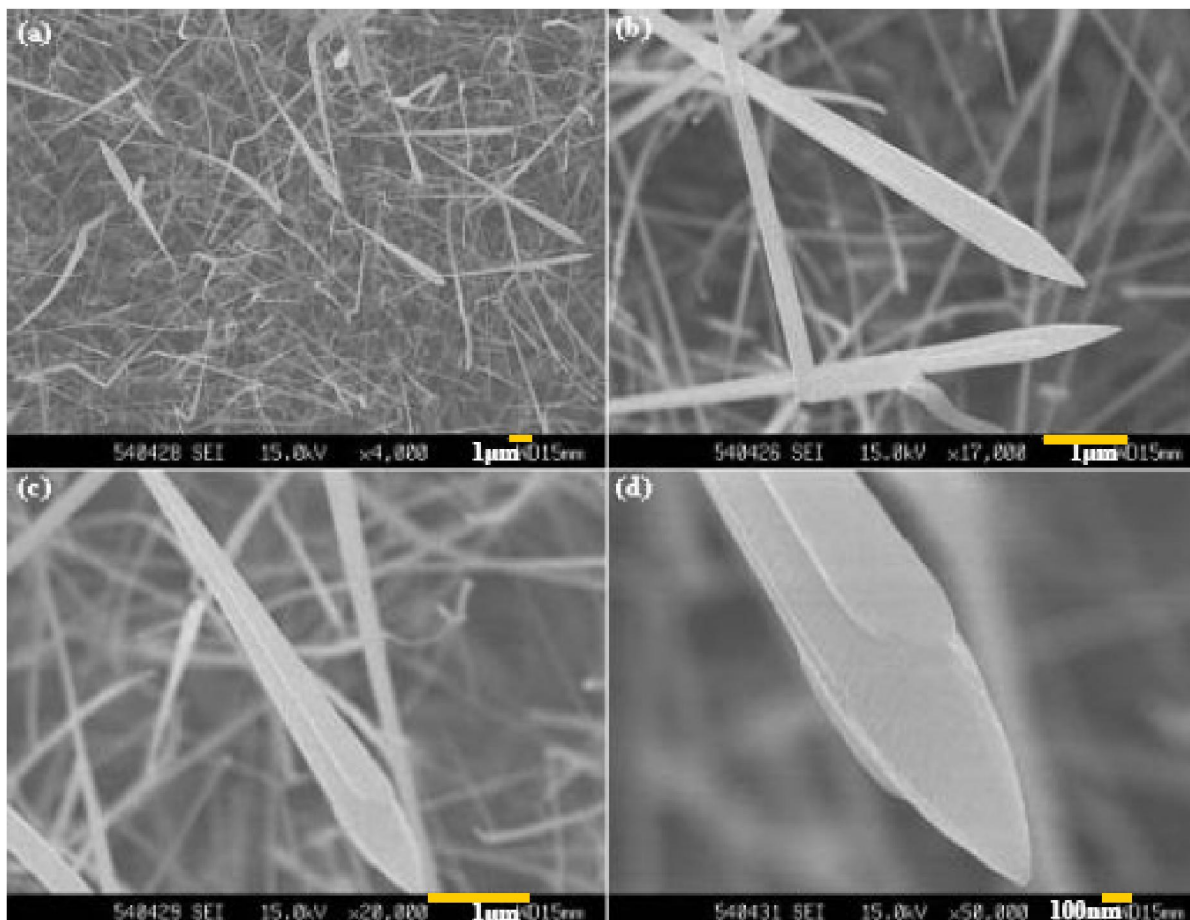


Figure 3 : FESEM morphologies (a), (b), (c), (d) of the synthesized SnO₂ nanopencils.

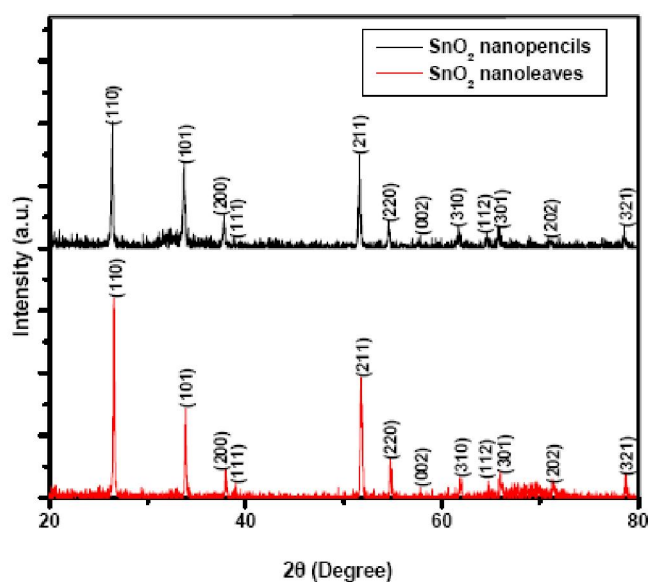


Figure 4: XRD pattern of the synthesized SnO₂ nanostructures.

Figure 5 depicts the room temperature Raman scattering spectra of two samples. Generally, rutile SnO₂ belongs to the space group D_{4h}^{14} , of which the normal lattice vibration at the \tilde{A} point of the Brillouin zone is given on the basis of group theory^[32]: $\tilde{A} = 1A_{1g} + 1A_{2g} + 1A_{2u} + 1B_{1g} + 1B_{2g} + 2B_{1u} + 1E_g + 3E_u$. Among them, the four first orders active Raman modes are B_{1g} , E_g , A_{1g} and B_{2g} , while the active IR modes are A_{2u} , E_u and B_{1u} . In the room temperature Raman scattering spectra (Figure 5) of the SnO₂ thin films, three fundamental Raman peaks at 470, 630 and 771 cm⁻¹ are appearance, which separately correspond to the E_g , A_{1g} and B_{2g} vibration modes^[33]. Thus, these peaks further confirm that the as-synthesized SnO₂ nanostructures possess the characteristic of the tetragonal rutile structure. In addition, the Raman band of 689 cm⁻¹ seem to correspond to A_{2u} LO (LO is the mode of the longitudinal

optical photos) modes, which is similar to $E_{u(2)}$ LO of SnO_2 nanorods^[14,34,35]. Furthermore, the peak at 540 cm^{-1} is identified to be of S_2 mode, which is believed to be the consequence of the disorder activation of SnO_2 nanoleaves^[36]. Subsequently, the peak at 578 cm^{-1} is identified to be of S_1 mode arising from surface region which, as an approximation, can be considered to be of constant thickness for two kinds of SnO_2 nanostructures^[37]. Finally, the peak at 520 cm^{-1} in the Raman spectrum of the SnO_2 nanopencils is the characteristic peak of the Si substrate, which indicate that the thickness and density of the nanostructures synthesized in substrate 1 are higher than those of the nanostructures synthesized in substrate 2, so that the Si peak does not appear in the Raman spectrum of SnO_2 nanoleaves.

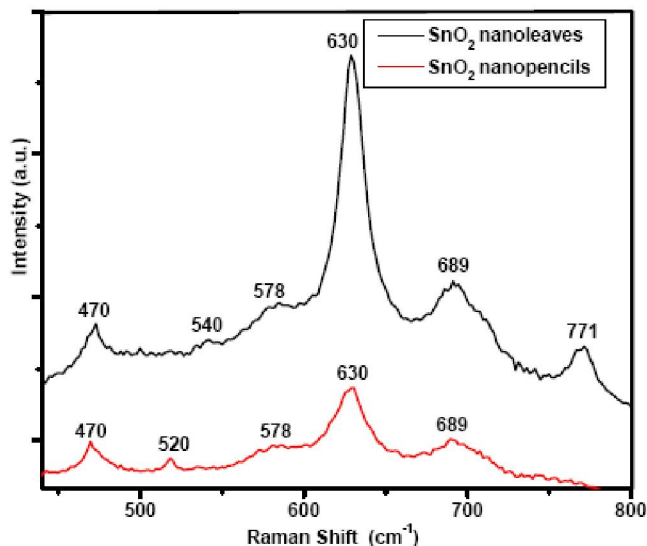


Figure 5: Raman spectrum of the synthesized SnO_2 nanostructures.

Photoluminescence of the obtained SnO_2 nanostructures are investigated at room temperature and the results are shown in Figure 6. The PL spectra consist of the emission band located at 343, 370, 399, 470 and 551 nm. Firstly, the peak at 343 nm is the band-to-band emission peak of the two kinds of SnO_2 nanostructures, which is originated from the recombination of free exciton electronhole^[38]. Notably, compared with its bulk counterpart (350 nm, $\sim 3.54\text{ eV}$), the peak at 343 nm shows a blue shift due to nanosize effect. The variational trend is consistent with other experimental observations, which is origin from perturbation of Hamiltonian due to size dependence of inter-

atomic potential^[39]. Also, the reason that the intensity of peak is weaker than those of other peaks is that the peaks caused by defect levels associated with oxygen vacancies or tin interstitials resulting from the size effect of the SnO_2 nanostructures is strong so as to cripple the band-to-band emission peak^[38]. Secondly, the 370 nm peak is attributed to the band-to-acceptor peak and related to the impurity or defect concentration and not to the structural properties^[40]. Thirdly, the appearance of the 399 nm peak is independent of the concentration of oxygen vacancies, while due to structural defects or luminescent centers, such as nanocrystals or defects in the SnO_2 thin films^[40,41]. Fourthly, the peak at 470 nm is possibly attributed to the electron transition mediated by defect levels such as oxygen vacancies in the band gap^[42]. Fifthly, the 551 nm peak has been observed in previous report^[43]. In addition, the PL spectra of the SnO_2 nanoleaves consist of the emission band located at 456 nm, which is newly found in our case. The reason of its appearance attributes to the new luminescence centers existing in SnO_2 nanoleaves, such as nanometer sized crystals and defects^[33].

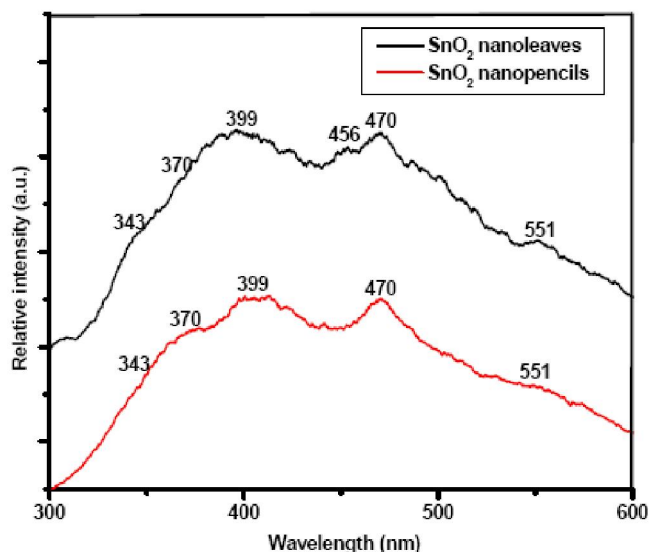


Figure 6: Room temperature PL spectrum of the synthesized SnO_2 nanostructures.

The growth mechanism of SnO_2 nanostructures can be explained on the basis of the vapor-liquid-solid (VLS) processes. In experimental, Au in Au-Ag alloy as catalysts is usually used to assist the SnO_2 nanostructures synthesis. SnO_2 powders firstly react with the active carbon, and then SnO can be produced. Subsequently, the produced SnO decomposes into Sn

Full Paper

and SnO₂. Sn droplets are still liquid at the reaction temperature due to the low melting point (231.9°C) and fall on the substrate, and then form alloyed droplets by reacting with the Au particles^[36]. Simultaneously, these alloying droplets can provide the energetically favored sites for the adsorption of SnO₂ vapor, so the SnO₂ dissolves in the alloying droplets. The continuous dissolution of SnO₂ results in a supersaturated solution^[44]. Ultimately, the SnO₂ nanostructures grow by precipitation of SnO₂ from the supersaturated droplets.

In addition, the different distance of substrates away from the source could lead to different temperature, which may be one of the main reasons for causing different morphologies of SnO₂ nanostructures. Physically, the diffusion behaviors of deposition atoms would largely influence on the geometrical shadowing. Evidently, there exists a diffusion barrier of deposited atoms, which is determined on the ambient conditions such as temperature, pressure and deposition flux in different incidence, etc^[45].

Moreover, the different supersaturating degree of alloying droplets plays an important role in the formation of different nanostructures^[46]. The theoretical calculations reveal that most stable crystal habit of SnO₂ is a tetragon elongated along the *c*-axis^[47]. Accordingly, SnO₂ have firstly optimized and secondly optimized growth directions. At higher temperature, the single crystal grows along the two optimized directions simultaneously. Moreover, the growth along the firstly optimized direction is faster than along the secondly optimized direction, so that the products such as 2D SnO₂ nanoleaves can be formed. At lower temperature, the single crystal grows along one of the two optimized directions to form 1D SnO₂ nanopencils in our experiment.

CONCLUSION

In summary, we have fabricated 2D nanoleaves and 1D nanopencils of SnO₂ on single silicon substrates by Au-Ag alloying catalyst assisted carbothermal evaporation. The band-to-band transition in the measured PL spectra indicates the blue shift of band gap due to nanosize effect. Meanwhile, the new peak at 456 nm in PL spectra is shown for SnO₂ nanoleaves,

implying that more luminescence centers exist in SnO₂ nanoleaves due to nanocrystals and defects. In terms of related considerations, the diffusion behavior of deposited atoms under different conditions and the different supersaturating degree of alloying droplets are suggested to play the crucial role in the shape growth. Also, the growth mechanism of the SnO₂ nanostructures is discussed on the basis of the vapor-liquid-solid (VLS) correlation. These nanostructures are expected to be applications in nano- and microelectronics and chemistry.

ACKNOWLEDGEMENTS

Project supported by the Scientific Research Fund of Hunan Provincial Education Department (No. 08B052), the National Natural Science Foundation of China (Nos. 10804030, 10704050), the Key Project of Chinese Ministry of Education (No. 209088), and the Cultivate outstanding young creative talents item for the university in Guangdong Province (No. LYM08088).

REFERENCES

- [1] A.M.Morales, C.M.Lieber; *Science*, **279**, 208 (1998).
- [2] Z.W.Pan, Z.R.Dai, Z.L.Wang; *Science*, **291**, 1947 (2001).
- [3] Y.Xia, P.D.Yang, Y.G.Sun, Y.Y.Wu, B.Mayers, B.Gates, Y.D.Yin, F.Kim, H.Q.Yan; *Adv.Mater.*, **15**, 353 (2003).
- [4] M.S.Park, G.X.Wang, Y.M.Kang, D.Wexler, S.X.Dou, H.K.Liu; *Angew.Chem.Int.Ed.*, **46**, 750 (2007).
- [5] S.Ferrere, A.Zaban, B.A.Gregg; *J.Phys.Chem.B*, **101**, 4490 (1997).
- [6] Y.S.He, J.C.Cambell, R.C.Murphy, M.F.Arendt, J.S.Swinnea; *J.Mater.Res.*, **8**, 3131 (1993).
- [7] G.Ansari, P.Boroojerdian, S.R.Sainkar, R.N.Karekar, R.C.Alyer, S.K.Kulkarni; *Thin Solid Films*, **295**, 271 (1997).
- [8] O.K.Varghese, L.K.Malhotra; *Sens.Actuat.B*, **53**, 19 (1998).
- [9] X.F.Duan, Y.Huang, Y.Cui, J.Wang, C.M.Lieber; *Nature*, **409**, 66 (2001).
- [10] E.R.Leite, I.T.Weber, E.Longo, J.A.Varela; *Adv.Mater.*, **12**, 965 (2000).

- [11] Y.Li, Y.H.Zhao, Z.H.Zhang, W.Liu, V.Ortalan, Y.Z.Zhou, X.L.Ma, E.J.Lavernia; *J.Crystal Growth*, **310**, 4226 (2008).
- [12] O.Lupan, L.Chow, G.Chai, H.Heinrich, S.Park, A.Schulte; *J.Crystal Growth*, **311**, 152 (2008).
- [13] S.Iijima; *Nature*, **375**, 769 (1991).
- [14] Y.K.Liu, C.L.Zheng, W.Z.Wang, C.R.Yin, G.H.Wang; *Adv.Mater.*, **13**, 1883 (2001).
- [15] Y.Feldman, E.Wasserman, D.J.Srolovitz, R.R.Tenne; *Science*, **267**, 222 (1995).
- [16] H.J.Dai, W.E.Wong, Y.Z.Yu, S.S.Fan, C.M.Lieber; *Nature*, **375**, 769 (1995).
- [17] Z.W.Pan, H.L.Lai, X.F.Duan, W.Y.Zhou, W.S.Shi, N.Wang, C.S.Lee, N.B.Wong, S.T.Lee, S.S.Xie; *Adv.Mater.*, **12**, 1186 (2000).
- [18] Z.L.Wang, Z.R.Dai, R.P.Gao, Z.G.Bai, J.L.Gole; *Appl.Phys.Lett.*, **77**, 3349 (2000).
- [19] W.Han, S.Fan, Q.Li, Y.Hu; *Science*, **277**, 1287 (1997).
- [20] X.F.Duan, C.M.Lieber; *J.Am.Chem.Soc.*, **122**, 188 (2000).
- [21] W.Q.Han, S.S.Fan, Q.Q.Li, B.L.Gu, X.B.Zhang, D.P.Yu; *Appl.Phys.Lett.*, **71**, 2271 (1997).
- [22] X.F.Duan, C.M.Lieber; *Adv.Mater.*, **12**, 298 (2000).
- [23] S.T.Lee, N.Wang, Y.F.Zhang, Y.H.Yang; *Mater.Res.Soc.Bulletin.*, **24**, 36 (1999).
- [24] B.Wang, G.Ouyang, Y.H.Yang, G.W.Yang; *Appl.Phys.Lett.*, **90**, 121905 (2007).
- [25] H.B.Zeng, W.P.Cai, Y.Li, J.L.Hu, P.S.Liu; *J.Phys.Chem.B*, **109**, 18260 (2005).
- [26] G.Ouyang, X.Tan, C.X.Wang, G.W.Yang; *Chem.Phys.Lett.*, **420**, 65 (2006).
- [27] G.Ouyang, X.Tan, C.X.Wang, G.W.Yang; *Chem.Phys.Lett.*, **423**, 143 (2006).
- [28] G.Ouyang, X.L.Li, G.W.Yang; *Phys.Rev.B*, **76**, 193406 (2007).
- [29] Y.Wu, B.Yang, B.Zong, H.Sun, Z.Shen, Y.Feng; *J.Mater.Chem.*, **14**, 469 (2004).
- [30] B.Wang, L.F.Zhu, Y.H.Yang, N.S.Xu, G.W.Yang; *J.Phys.Chem.C*, **112**, 6643 (2008).
- [31] H.Huang, O.K.Tan, Y.C.Lee, M.S.Tse, J.Guo, T.White; *Nanotechnology*, **17**, 743 (2006).
- [32] S.P.S.Porto, P.A.Fleury, T.C.Damen; *Phys.Rev.*, **154**, 522 (1967).
- [33] S.H.Sun, G.W.Meng, G.X.Zhang, T.Gao, B.Y.Geng, L.D.Zhang, J.Zuo; *Chem.Phys.Lett.*, **376**, 103 (2003).
- [34] X.S.Peng, L.D.Zhang, G.W.Meng, Y.T.Tian, Y.Lin, B.Y.Geng, S.H.Sun; *Vacuum*, **93**, 1760 (2003).
- [35] L.Abello, B.Bochu, A.Gaskov, S.Koudryavtseva, G.Lucazeau, M.Roumyantesva; *J.Solid State Chem.*, **135**, 78 (1998).
- [36] J.X.Wang, D.F.Liu, X.Q.Yan, H.J.Yuan, L.J.Ci, Z.P.Zhou, Y.Gao, L.Song, L.F.Liu, W.Y.Zhou, G.Wang, S.S.Xie; *Solid.State Commun.*, **130**, 89 (2004).
- [37] A.Dieguez, A.R.Rodrigues, A.Vila, J.R.Morante; *J.Appl.Phys.*, **90**, 1550 (2001).
- [38] E.J.H.Lee, C.Ribeiro, T.R.Giraldi, E.Longo, E.R.Leite; *Appl.Phys.Lett.*, **84**, 1745 (2004).
- [39] Y.Wang, G.Ouyang, L.L.Wang, L.M.Dang, D.S.Dang, C.Q.Sun; *Chem.Phys.Lett.*, **463**, 383 (2008).
- [40] J.Jeong, S.P.Choi, C.Chang, D.C.Shin, J.S.Park, B.T.Lee, Y.J.Park, H.J.Song; *Solid State Commun.*, **127**, 595 (2003).
- [41] T.W.Kimand, D.U.Lee; *J.Appl.Phys.*, **88**, 3759 (2000).
- [42] F.Gu, S.F.Wang, M.K.Lu, G.J.Zhou, D.Xu, D.R.Yuan; *J.Phys.Chem.B*, **108**, 8119 (2004).
- [43] B.Wang, Y.H.Yang, C.X.Wang, G.W.Yang; *Chem.Phys.Lett.*, **407**, 347 (2005).
- [44] Y.Q.Chen, X.F.Cui, K.Zheng, D.Y.Pan, S.Y.Zhang, B.Wang, J.G.Hou; *Chem.Phys.Lett.*, **369**, 16 (2003).
- [45] L.G.Zhou, H.C.Huang; *Phys.Rev.Lett.*, **101**, 266102 (2008).
- [46] A.P.Levitt; *Whisker Technology*, Wiley, New York, (1970).
- [47] S.H.Sun, G.W.Meng, M.G.Zhang, X.H.An, G.S.Wu, L.D.Zhang; *J.Phys.D: Appl.Phys.*, **37**, 409 (2004).